

Modulation of photothermal degradation of epoxy upon ultraviolet irradiation by polyhedral oligomeric silsesquioxane : A multiscale simulation study

Youngoh Kim^{a,b} and Joonmyung Choi^{a,b,}*

^aDepartment of Mechanical Design Engineering, Hanyang University, 222 Wangsimni-ro, Seongdong-gu, Seoul 04763, Korea

^bDepartment of Mechanical Engineering, BK21 FOUR ERICA-ACE Center, Hanyang University, 55 Hanyangdaehak-ro, Sangnok-gu Ansan 15588, Korea

Corresponding author

E-mail address: joonchoi@hanyang.ac.kr

Supporting Information

Appendix A

All-atom MD simulations were performed using the LAMMPS open-source code integrated with the *Class 2* package.^{S1, S2} The force-field parameters used for calculating the interatomic potential energy followed the PCFF developed by H. Sun.^{S2} The PCFF describes the molecular potential energy using Taylor expansion in the stretching, bending, torsion, out-of-plane bending, and other cross-coupling terms of the optimized structure as follows:

$$U_{total} = E_s + E_b + E_t + E_o + E_{ss} + E_{sb} + E_{vdW} + E_{Coulomb} \quad \text{Eq. S1}$$

$$E_s = \sum_{n=2}^4 k_n^s (l - l_0)^n \quad \text{Eq. S2-1}$$

$$E_b = \sum_{n=2}^4 k_n^b (\theta - \theta_0)^n \quad \text{Eq. S2-2}$$

$$E_t = \sum_{n=1}^3 k_n^t (1 - \cos n\varphi) \quad \text{Eq. S2-3}$$

$$E_o = k^o (\chi - \chi_0)^2 \quad \text{Eq. S2-4}$$

$$E_{ss} = k^{ss} (l - l_0) (l' - l'_0) \quad \text{Eq. S2-5}$$

$$E_{sb} = k_1^{sb} (l - l_0) (\theta - \theta_0) + k_2^{sb} (l' - l'_0) (\theta - \theta_0) \quad \text{Eq. S2-6}$$

$$E_{vdW} = \varepsilon_{ij} \left[2 \left(\frac{\sigma_{ij}}{r_{ij}} \right)^9 - 3 \left(\frac{\sigma_{ij}}{r_{ij}} \right)^6 \right] \quad \text{Eq. S2-7}$$

$$E_{Coulomb} = \frac{Q_i Q_j}{r_{ij}} \quad \text{Eq. S2-8}$$

$$\varepsilon_{ij} = \frac{2\sqrt{\varepsilon_i \varepsilon_j} \sigma_i^3 \sigma_j^3}{\sigma_i^6 + \sigma_j^6} \quad \text{Eq. S3-1}$$

$$\sigma_{ij} = \left(\frac{1}{2} (\sigma_i^6 + \sigma_j^6) \right)^{\frac{1}{6}} \quad \text{Eq. S3-2}$$

where E_s , E_b , E_t , and E_o are the potential energies associated with bond stretching, angular bending, dihedral torsion, and planar bending deformation, respectively; E_{ss} , and E_{sb} are the

cross-coupled potential energies induced by two-bond stretching and stretch-bend coupling, respectively; E_{vdW} , and $E_{Coulomb}$ are the van der Waals dispersion and Coulombic electrostatic interactions, respectively. All the coefficients ($k_n^s, k_n^b, k_n^t, k^0, k^{ss}, k^{sb}$) are constants calculated theoretically from the n^{th} -order derivatives of the potential energy surfaces, as obtained from Taylor expansion. The parameters l_0, θ_0 , and χ_0 are the bond length, valence angle, and torsional angle that satisfy $\frac{\partial U(\alpha_0)}{\partial \alpha} = 0$ ($\alpha = l, \theta, \text{ and } \chi$); ε_i, σ_i , and Q_i are the dispersion coefficient, self-equilibrium distance, and point charge on atom i . The force-field parameters used in this study are provided in **Tables SI-SVII**. The crosslinked epoxy and epoxy/POSS nanocomposite models were prepared as follows. First, 90 molecules of DETDA and 45 molecules of DGEBA were randomly filled into a periodic unit cell of $8.5 \times 8.5 \times 8.5 \text{ nm}^3$ (**Figure S1a**). To prevent undesired intermolecular interference, the density of the unit cell was very low at 0.1 g/cc, and then the cell size was gradually reduced until the density reached 0.98 g/cc. The geometry of the molecules constituting the unit cell was optimised using the conjugated gradient method. Subsequently, epoxy networks were constructed using a crosslinking reaction simulation process (**Figure S1b**). The nitrogen atoms at both amine groups of DETDA were assigned as lone pair donors, and the carbon atoms at the ends of the epoxide group were assigned as lone pair acceptors. For all the polymeric molecules inside the unit cell, the nearest distance from the lone pair donor site to the acceptor site was calculated. If the distance was within the specified cutoff range, epoxide ring opening, hydroxyl group formation, and C–N covalent bond formation were sequentially performed to simulate an amine–epoxy reaction. The abrupt potential energy changes caused by the formation and removal of covalent bonds were relaxed during the short equilibrium that employed NVT ensembles at 300 K for 30 ps. When all the epoxy resins were crosslinked, the reaction cutoff

value slightly increased at 0.2 Å intervals. This process was repeated until the crosslinking rate of the epoxy resin inside the unit cell reached 70%. While updating the cutoff distance for the crosslinking reaction, self-assisted polymerisation with a C-N distance of 1.754 Å and non-catalysed polymerisation with a C-N distance of 3.387 Å were considered sequentially.^{S3} Finally, an equilibrium structure was obtained by applying the NPT ensemble at room temperature and atmospheric pressure for 5 ns. The integration of the equations of motion was achieved with a time step of 1 fs.

The epoxy/POSS nanocomposite model was constructed in the same method as the crosslinked neat epoxy model, except that four POSS molecules were inserted together as fillers. Octa(3-Glycidyl)propoxy POSS was considered, and in the simulation process, the epoxide constituting the substituents of POSS participated in the reaction preferentially over DGEBF. After the equilibration process at room temperature and atmospheric pressure conditions was completed, the densities of the neat epoxy model and the epoxy/POSS nanocomposites model were 1.12 and 1.14 g/cc, respectively (**Figure S1c**). The density of neat epoxy obtained from MD simulations is significantly in line with the density of 1.19 g/cc measured in the study done by Odegard et al. (**Figure S5a**).^{S4}

The model constructed from the MD simulations was also validated using the prediction of the glass transition temperature of the system. The glass transition temperature of neat epoxy was predicted using the cool-down simulations. Under the NPT ensemble, the system temperature was raised to 550 K, and then lowered to room temperature at a cooling rate of 20 K/ns to track the change in density. The results show a sharp change in density around 425 K (**Figure S5b**), thus suggesting that near this point is the glass transition temperature of the system, which is similar to the well-known glass transition temperature of neat epoxy (423 K).^{S5}

Uniaxial tensile loading simulations were conducted under the NPT ensemble at 1 K and atmospheric pressure conditions to investigate the structural mechanics of the epoxy/POSS network. The unit cells were elongated at a strain rate of 10^6 /s until the total strain reached 0.3%. The application of extremely low temperatures minimises the undesired thermal fluctuations of atoms, allowing the analysis of the role of each molecular component from a purely mechanical perspective.^{S6} It should also be noted that the strain rate applied in this study is a condition commonly used to evaluate the mechanical properties of the all-atom system in the elastic deformation region.^{S6-S8}

Appendix B

Photothermal reaction-induced thermodynamics was implemented to explore the UV degradation effect in the classical MD framework. First, the vibrational energy of the normal mode activated under the electronic state transition was calculated to account for the vibrationally excited state. The kinetic energy corresponding to the vibration was forcibly injected into the atoms involving the activated normal mode. At this stage, both vibrational excitation and non-radiative decay processes are described. By defining the chromophore group excitation probability as 100%, we took into account the fact that both adsorption- and emission-induced vibrations between the excited and ground states are inherent. Energy injection was performed every 10 ps during the MD run. Some covalent bonds exceeding the bond dissociation energy were detected in the intramolecular vibrations triggered by the locally increased kinetic energy and subsequent energy dissipation. These covalent bonds were removed during the MD run, and the force-field parameters of the relevant atoms were immediately updated. The bond dissociation energy determines the scission of the bonds, as shown in **Table SVIII**. During the integration of photothermal reaction-induced

thermodynamics, a quantum thermal bath was adopted as a thermostat to ensure molecular vibration characteristics through colored noise.^{S9-S14}

Appendix C

The photochemical processes and vibrational excitation of DETDA, DGEBF, and POSS were explored using TD-DFT with the GAMESS code.^{S15} The optimised geometries of each molecule in the ground state were obtained with a force tolerance of 1×10^{-8} eV/Å, and the ten lowest-lying singlet states were considered to calculate the transition energy using the B3LYP/6-31G(d)+ level of theory.^{S16, S17} In addition, the Franck-Condon factors (Γ_{if}) were employed to analyse the vibrational excited state as follows:

$$\Gamma_{if} = \mu_{if}(r)^2 (\langle \varphi_f(R) | \varphi_i(R) \rangle)^2 \quad \text{Eq. S4}$$

where μ_{if} is the electronic transition dipole moment from state i to f ; φ_i and φ_f are the vibrational wavefunctions of states i and f , respectively; r and R are the electronic and nuclear coordinates, respectively. The intrachain energy dissipation during nonradiative decay was investigated using the frequency-analysis-based energy transfer kinetics proposed by Kim and Choi.^{S18} To quantify the frequency of the stretching mode, the normal mode and its corresponding frequency of DETDA, DGEBF, and POSS were calculated using DFT at the B3LYP/6-31G(d)+ level of theory.^{S16, S17}

All classical MD simulations and DFT calculations were conducted in a workstation with

Table SI Force-field parameters used for describing interatomic bond stretching. The units of k^S and l_0 are kcal/mol and Å, respectively.

$i - j$	l_0	K_2^S	K_3^S	K_4^S
$C_{aromatic} - C_{aromatic}$	1.417	470.8361	-627.618	1327.635
$C_{aromatic} - C_{alkane}$	1.501	321.9021	-521.821	572.1628
$C_{aromatic} - H$	1.0982	372.8251	-803.453	894.3173
$C_{aromatic} - O_{ether}$	1.3768	428.8798	-738.235	1114.966
$C_{aromatic} - N_{amine}$	1.3912	447.0438	-784.535	886.1671
$C_{aromatic} - C_{methyl}$	1.501	321.9021	-521.821	572.1628
$C_{alkane} - C_{alkane}$	1.53	299.67	-501.77	679.81
$C_{alkane} - H$	1.101	345.0	-691.89	844.6
$C_{alkane} - O_{ether}$	1.42	400.3954	-835.195	1313.014
$C_{alkane} - C_{alkane}^*$	1.53	299.67	-501.77	679.81
$C_{alkane} - N_{amine}$	1.3912	447.0438	-784.535	886.1671
$C_{alkane} - C_{methyl}$	1.53	299.67	-501.77	679.81
$C_{alkane} - Si_{POSS}$	1.9073	157.0049	-237.02	356.0328
$C_{alkane} - C_{epoxide}$	1.53	299.67	-501.77	679.81
$C_{alkane}^* - H$	1.101	345.0	-691.89	844.6
$C_{alkane}^* - O_{hydroxyl}$	1.42	400.3954	-835.195	1313.014
$C_{methyl} - H$	1.101	345.0	-691.89	844.6
$C_{epoxide} - C_{epoxide}$	1.53	299.67	-501.77	679.81
$C_{epoxide} - O_{epoxide}$	1.42	400.3954	-835.195	1313.014
$C_{epoxide} - H$	1.101	345.0	-691.89	844.6

$O_{hydroxyl} - H_{hydroxyl}$	0.965	532.5062	-1282.91	2004.766
$N_{amine} - H$	1.0012	465.8608	-1066.24	1496.565
$Si_{POSS} - O_{POSS}$	1.6562	306.1232	-517.342	673.7067

*: One hydrogen is substituted with a heavy element such as a halogen or oxygen.

Table SII Force-field parameters used for describing valence-angle bending. The units of k^b and θ_0 are kcal/mol and degrees, respectively.

$i - j - k$	θ_0	K_2^b	K_3^b	K_4^b
$C_{ar.} - C_{ar.} - C_{ar.}$	118.9	61.0226	-34.9931	0.0000
$C_{ar.} - C_{ar.} - C_{al.}$	120.05	44.7148	-22.7352	0.0000
$C_{ar.} - C_{ar.} - H$	117.94	35.1558	-12.4682	0.0000
$C_{ar.} - C_{ar.} - O_{et.}$	123.42	73.6781	-21.6787	0.0000
$C_{ar.} - C_{al.} - C_{ar.}$	111.0	44.3234	-9.4454	0.0000
$C_{ar.} - C_{al.} - H$	111.0	44.3234	-9.4454	0.0000
$H - C_{al.} - H$	107.66	39.641	-12.9210	-2.4318
$C_{ar.} - O_{et.} - C_{al.}$	102.9695	38.9739	-6.2595	-8.1710
$H - C_{al.} - O_{et.}$	108.728	58.5446	-10.8088	-12.4006
$O_{et.} - C_{al.} - C_{al.}^*$	111.27	54.5381	-8.3642	-13.0838
$H - C_{al.} - C_{al.}^*$	110.77	41.453	-10.604	5.129
$C_{al.} - C_{al.}^* - H$	110.77	41.453	-10.604	5.129
$C_{al.} - C_{al.}^* - C_{al.}$	112.67	39.516	-7.443	-9.5583
$C_{al.} - C_{al.}^* - O_{hy.}$	111.27	54.5381	-8.3642	-13.0838
$H - C_{al.}^* - O_{hy.}$	108.728	58.5446	-10.8088	-12.4006
$C_{al.}^* - C_{al.} - N_{am.}$	114.3018	42.6589	-10.5464	-9.3243
$H - C_{al.} - N_{am.}$	108.9372	57.401	2.9374	0.0000
$C_{al.}^* - O_{hy.} - H$	105.8	52.7061	-12.109	-9.8681
$C_{ar.} - C_{ar.} - N_{am.}$	121.4584	61.0647	-21.6172	0.0000

$C_{ar.} - C_{ar.} - C_{me.}$	120.05	44.7148	-22.7352	0.0000
$C_{ar.} - N_{am.} - C_{al.}$	106.01	109.7746	-9.0636	0.0000
$C_{al.} - N_{am.} - C_{al.}$	112.4436	47.2337	-10.6612	-10.2062
$C_{ar.} - C_{al.} - C_{me.}$	108.4	43.9594	-8.3924	-9.3379
$H - C_{al.} - C_{me.}$	110.77	41.453	-10.604	5.129
$C_{ar.} - C_{me.} - H$	111.0	44.3234	-9.4454	0.0000
$H - C_{me.} - H$	107.66	39.641	-12.921	-2.4318
$C_{al.} - C_{me.} - H$	110.77	41.453	-10.604	5.129
$O_{P.} - Si_{P.} - O_{P.}$	110.693	70.3069	-6.9375	0.0000
$C_{al.} - Si_{P.} - O_{P.}$	114.906	23.0218	-31.3993	24.9814
$Si_{P.} - O_{P.} - Si_{P.}$	157.026	9.074	-19.5576	8.500
$H - C_{al.} - Si_{P.}$	111.536	30.2481	-15.5255	0.0000
$C_{al.} - C_{al.} - Si_{P.}$	112.67	39.516	-7.443	0.0000
$C_{al.} - C_{al.} - H$	110.77	41.453	-10.604	5.129
$C_{al.} - C_{al.} - O_{et.}$	111.27	54.5381	-8.3642	-13.0838
$C_{al.} - O_{et.} - C_{al.}$	104.5	35.7454	-10.0067	-6.2729
$O_{et.} - C_{al.} - C_{ep.}$	111.27	54.5381	-8.3642	-13.0838
$H - C_{al.} - C_{ep.}$	110.77	41.453	-10.604	5.129
$C_{al.} - C_{ep.} - H$	110.77	41.453	-10.604	5.129
$C_{al.} - C_{ep.} - C_{ep.}$	112.67	39.516	-7.443	-9.5583
$C_{al.} - C_{ep.} - O_{ep.}$	111.27	54.5381	-8.3642	-13.0838
$H - C_{ep.} - C_{ep.}$	110.77	41.453	-10.604	5.129
$H - C_{ep.} - O_{ep.}$	108.728	58.5446	-10.8088	-12.4006
$C_{ep.} - C_{ep.} - O_{ep.}$	111.27	54.5381	-8.3642	-13.0838
$H - C_{ep.} - H$	107.66	39.641	-12.921	-2.4318
$C_{ep.} - O_{ep.} - C_{ep.}$	104.5	35.7454	-10.0067	-6.2729
$C_{ar.} - N_{am.} - H$	111.8725	40.8369	-15.6673	0.0000
$C_{al.} - N_{am.} - H$	111.8725	40.8369	-15.6673	0.0000
$H - N_{am.} - H$	107.5130	42.5182	-21.7566	-4.3372

*: One hydrogen is substituted with a heavy element such as a halogen or oxygen.

Table SIII Force-field parameters used for describing dihedral torsion. The unit of k^t is kcal/mol.

$i - j - k - l$	K_1^t	K_2^t	K_3^t
$C_{ar.} - C_{ar.} - C_{ar.} - C_{ar.}$	8.3667	1.1932	0.0000
$C_{ar.} - C_{ar.} - C_{ar.} - H$	0.0000	3.9661	0.0000
$C_{ar.} - C_{ar.} - C_{ar.} - C_{al.}$	0.0000	4.4072	0.0000
$C_{al.} - C_{ar.} - C_{ar.} - H$	0.0000	1.559	0.0000
$C_{ar.} - C_{ar.} - C_{al.} - C_{ar.}$	-0.2802	-0.0678	-0.0122
$C_{ar.} - C_{ar.} - C_{al.} - H$	-0.2801	-0.0678	-0.0122
$H - C_{ar.} - C_{ar.} - H$	0.0000	1.8769	0.0000
$C_{ar.} - C_{ar.} - C_{ar.} - O_{et.}$	0.0000	4.8498	0.0000
$H - C_{ar.} - C_{ar.} - O_{et.}$	0.0000	1.7234	0.0000
$C_{ar.} - C_{ar.} - O_{et.} - C_{al.}$	0.0000	1.500	0.0000
$H - C_{al.} - O_{et.} - C_{ar.}$	0.9513	0.1155	0.0720
$C_{al.}^* - C_{al.} - O_{et.} - C_{ar.}$	-0.5203	-0.3028	-0.345
$O_{et.} - C_{al.} - C_{al.}^* - H$	-0.1435	0.253	-0.0905
$O_{et.} - C_{al.} - C_{al.}^* - C_{al.}$	0.7137	0.266	-0.2545
$O_{et.} - C_{al.} - C_{al.}^* - O_{hy.}$	-0.182	-0.1084	-0.7047
$H - C_{al.} - C_{al.}^* - H$	-0.1432	0.0617	-0.1083
$H - C_{al.} - C_{al.}^* - C_{al.}$	0.0000	0.0316	-0.1681
$H - C_{al.} - C_{al.}^* - O_{hy.}$	-0.1435	0.253	-0.0905

$N_{am.} - C_{al.} - C_{al.}^* - C_{al.}$	0.0972	0.0722	-0.2581
$N_{am.} - C_{al.} - C_{al.}^* - H$	-0.0228	0.028	-0.1863
$N_{am.} - C_{al.} - C_{al.}^* - O_{hy.}$	-0.182	-0.1084	-0.7047
$C_{al.} - C_{al.}^* - O_{hy.} - H$	-0.6732	-0.4778	-0.167
$H - C_{al.}^* - O_{hy.} - H$	0.1863	-0.4338	-0.2121
$C_{al.}^* - C_{al.} - N_{am.} - C_{ar.}$	-0.0017	-0.0072	0.0008
$C_{al.}^* - C_{al.} - N_{am.} - H$	-0.0483	-0.0077	-0.0014
$H - C_{al.} - N_{am.} - C_{ar.}$	0.0406	0.0354	-0.1649
$H - C_{al.} - N_{am.} - H$	-0.0148	-0.0791	-0.0148
$C_{al.}^* - C_{al.} - N_{am.} - C_{al.}$	-0.0017	-0.0072	0.0008
$H - C_{al.} - N_{am.} - C_{al.}$	0.0406	0.0354	-0.1649
$C_{ar.} - C_{ar.} - C_{ar.} - N_{am.}$	0.0000	5.3826	0.0000
$C_{al.} - C_{ar.} - C_{ar.} - N_{am.}$	0.0972	0.0722	-0.2581
$C_{ar.} - C_{ar.} - C_{ar.} - C_{me.}$	0.0000	4.4072	0.0000
$N_{am.} - C_{ar.} - C_{ar.} - C_{me.}$	0.0972	0.0722	-0.2581
$C_{ar.} - C_{ar.} - N_{am.} - C_{al.}$	-0.0017	-0.0072	0.0008
$C_{ar.} - C_{ar.} - C_{al.} - C_{me.}$	-0.2802	-0.0678	-0.0122
$C_{ar.} - C_{ar.} - C_{me.} - H$	-0.2801	-0.0678	-0.0122
$C_{ar.} - C_{al.} - C_{me.} - H$	-0.0228	0.0280	-0.1863
$H - C_{al.} - C_{me.} - H$	-0.1432	0.0617	-0.1083
$O_p. - Si_p. - O_p. - Si_p.$	0.3000	0.3658	0.0000
$C_{al.} - Si_p. - O_p. - Si_p.$	0.0000	0.0000	-0.1300
$H - C_{al.} - Si_p. - O_p.$	-1.3513	0.0000	-0.0580
$C_{al.} - C_{al.} - Si_p. - O_p.$	-1.3513	0.0000	-0.0580
$H - C_{al.} - C_{al.} - Si_p.$	0.0000	0.6250	0.0000
$O_{et.} - C_{al.} - C_{al.} - Si_p.$	0.0000	0.6250	0.0000
$H - C_{al.} - C_{al.} - H$	-0.1432	0.0617	-0.1083
$H - C_{al.} - C_{al.} - O_{et.}$	-0.1435	0.2530	-0.0905
$C_{al.} - C_{al.} - O_{et.} - C_{al.}$	-0.5203	-0.3028	-0.3450
$H - C_{al.} - O_{et.} - C_{al.}$	0.5302	0.0000	-0.3966
$C_{al.}^* - C_{al.} - O_{et.} - C_{al.}$	-0.5203	-0.3028	-0.3450
$C_{ep.} - C_{al.} - O_{et.} - C_{ar.}$	0.0000	0.9000	0.0000

$O_{et.} - C_{al.} - C_{ep.} - H$	-0.1435	0.2530	-0.0905
$O_{et.} - C_{al.} - C_{ep.} - C_{ep.}$	0.7137	0.2660	-0.2545
$O_{et.} - C_{al.} - C_{ep.} - O_{ep.}$	-0.1820	-0.1084	-0.7047
$H - C_{al.} - C_{ep.} - H$	-0.1432	0.0617	-0.1083
$H - C_{al.} - C_{ep.} - C_{ep.}$	0.0000	0.0316	-0.1681
$H - C_{al.} - C_{ep.} - O_{ep.}$	-0.1435	0.2530	-0.0905
$C_{al.} - C_{ep.} - C_{ep.} - H$	0.0000	0.0316	-0.1681
$C_{al.} - C_{ep.} - C_{ep.} - O_{ep.}$	0.7137	0.2660	-0.2545
$H - C_{ep.} - C_{ep.} - H$	-0.1432	0.0617	-0.1083
$H - C_{ep.} - C_{ep.} - O_{ep.}$	-0.1435	0.2530	-0.0905
$C_{al.} - C_{ep.} - O_{ep.} - C_{ep.}$	-0.5203	-0.3028	-0.3450
$H - C_{ep.} - O_{ep.} - C_{ep.}$	0.5302	0.0000	-0.3966
$C_{ar.} - C_{ar.} - N_{am.} - H$	0.0000	1.2190	0.0000

*: One hydrogen is substituted with a heavy element such as a halogen or oxygen.

Table SIV Force-field parameters used for describing planar bending. The unit of k^o is kcal/mol.

$i - j - k - l$	K^o
$C_{ar.} - C_{ar.} - C_{ar.} - C_{al.}$	7.8153
$C_{ar.} - C_{ar.} - C_{ar.} - H$	4.8912
$C_{ar.} - C_{ar.} - C_{ar.} - O_{et.}$	13.0421
$C_{al.} - C_{ar.} - C_{ar.} - N_{am.}$	10.7855
$C_{ar.} - C_{ar.} - C_{al.} - C_{me.}$	7.8153

Table SV Force-field parameters used for describing bond-bond cross-coupled terms. The unit of k^{SS} is kcal/mol $\cdot \text{\AA}^2$ and that of l_0 and l_0' is \AA .

$i - j - k$	k^{SS}	l_0	l_0'
$C_{ar.} - C_{ar.} - C_{ar.}$	68.2856	1.417	1.417
$C_{ar.} - C_{ar.} - C_{al.}$	12.0676	1.417	1.501
$C_{ar.} - C_{ar.} - H$	1.0795	1.417	1.0982
$C_{ar.} - C_{ar.} - O_{et.}$	48.4754	1.417	1.3768
$C_{ar.} - C_{al.} - C_{ar.}$	0.0000	1.501	1.501
$C_{ar.} - C_{al.} - H$	2.9168	1.501	1.101
$H - C_{al.} - H$	5.3316	1.101	1.101
$C_{ar.} - O_{et.} - C_{al.}$	0.0000	1.3768	1.42
$H - C_{al.} - O_{et.}$	23.1979	1.101	1.42
$O_{et.} - C_{al.} - C_{al.}^*$	11.4318	1.42	1.53
$H - C_{al.} - C_{al.}^*$	3.3872	1.101	1.53
$C_{al.} - C_{al.}^* - H$	3.3872	1.53	1.101
$C_{al.} - C_{al.}^* - C_{al.}$	0.000	1.53	1.53
$C_{al.} - C_{al.}^* - O_{hy.}$	11.4318	1.53	1.42
$H - C_{al.}^* - O_{hy.}$	23.1979	1.101	1.42
$C_{al.}^* - C_{al.} - N_{am.}$	0.0000	1.53	0.0000
$H - C_{al.} - N_{am.}$	0.0000	1.101	0.0000

$C_{al.}^* - O_{hy.} - H$	-9.6879	1.42	0.965
$C_{ar.} - C_{ar.} - N_{am.}$	46.9513	1.417	1.3912
$C_{ar.} - C_{ar.} - C_{me.}$	12.0676	1.417	1.501
$C_{ar.} - N_{am.} - C_{al.}$	0.0000	1.3912	0.0000
$C_{al.} - N_{am.} - C_{al.}$	0.0000	0.0000	0.0000
$C_{ar.} - C_{al.} - C_{me.}$	0.0000	1.5010	1.53
$H - C_{al.} - C_{me.}$	3.3872	1.101	1.53
$C_{ar.} - C_{me.} - H$	2.9168	1.501	1.1010
$H - C_{me.} - H$	5.3316	1.101	1.101
$C_{al.} - C_{me.} - H$	3.3872	1.53	1.101
$O_{P.} - Si_{P.} - O_{P.}$	41.1143	1.6562	1.6562
$C_{al.} - Si_{P.} - O_{P.}$	5.4896	1.9073	1.6562
$Si_{P.} - O_{P.} - Si_{P.}$	41.1143	1.6562	1.6562
$H - C_{al.} - Si_{P.}$	6.382	1.101	1.9073
$C_{al.} - C_{al.} - Si_{P.}$	0.0000	1.53	1.9073
$C_{al.} - C_{al.} - H$	3.3872	1.53	1.1010
$C_{al.} - C_{al.} - O_{et.}$	11.4318	1.53	1.42
$C_{al.} - O_{et.} - C_{al.}$	-7.1131	1.42	1.42
$O_{et.} - C_{al.} - C_{ep.}$	11.4318	1.42	1.53
$H - C_{al.} - C_{ep.}$	3.3872	1.101	1.53
$C_{al.} - C_{ep.} - H$	3.3872	1.53	1.101
$C_{al.} - C_{ep.} - C_{ep.}$	0.0000	1.53	1.53
$C_{al.} - C_{ep.} - O_{ep.}$	11.4318	1.53	1.42
$H - C_{ep.} - C_{ep.}$	3.3872	1.101	1.53
$H - C_{ep.} - O_{ep.}$	23.1979	1.101	1.42
$C_{ep.} - C_{ep.} - O_{ep.}$	11.4318	1.53	1.42
$H - C_{ep.} - H$	5.3316	1.101	1.101
$C_{ep.} - O_{ep.} - C_{ep.}$	-7.1131	1.42	1.42
$C_{ar.} - N_{am.} - H$	4.5393	1.3912	1.0012
$C_{al.} - N_{am.} - H$	0.0000	0.0000	1.0012
$H - N_{am.} - H$	-9.9447	1.0012	1.0012

*: One hydrogen is substituted with a heavy element such as a halogen or oxygen.

Table SVI Force-field parameters used for describing bond-angle cross-coupled terms. The unit of k^{sb} is kcal/mol \cdot Å, and that of l_0 and l'_0 is Å.

$i - j - k$	k_1^{sb}	k_2^{sb}	l_0	l'_0
$C_{ar.} - C_{ar.} - C_{ar.}$	28.8708	28.8708	1.417	1.417
$C_{ar.} - C_{ar.} - C_{al.}$	31.0771	47.0579	1.417	1.501
$C_{ar.} - C_{ar.} - H$	20.0033	24.2183	1.417	1.0982
$C_{ar.} - C_{ar.} - O_{et.}$	58.4790	107.6806	1.417	1.3768
$C_{ar.} - C_{al.} - C_{ar.}$	0.0000	0.0000	1.501	1.501
$C_{ar.} - C_{al.} - H$	26.4608	11.7717	1.501	1.101
$H - C_{al.} - H$	18.103	18.103	1.101	1.101
$C_{ar.} - O_{et.} - C_{al.}$	0.0000	0.0000	1.3768	1.42
$H - C_{al.} - O_{et.}$	4.6189	55.327	1.101	1.42
$O_{et.} - C_{al.} - C_{al.}^*$	20.4033	2.6868	1.42	1.53
$H - C_{al.} - C_{al.}^*$	11.421	20.754	1.101	1.53
$C_{al.} - C_{al.}^* - H$	20.754	11.421	1.53	1.101
$C_{al.} - C_{al.}^* - C_{al.}$	8.016	8.016	1.53	1.53
$C_{al.} - C_{al.}^* - O_{hy.}$	2.6868	20.4033	1.53	1.42
$H - C_{al.}^* - O_{hy.}$	4.6189	55.327	1.101	1.42
$C_{al.}^* - C_{al.} - N_{am.}$	0.0000	0.0000	1.53	0.0000

$H - C_{al.} - N_{am.}$	0.0000	0.0000	1.101	0.0000
$C_{al.}^* - O_{hy.} - H$	28.58	18.9277	1.42	0.965
$C_{ar.} - C_{ar.} - N_{am.}$	39.404	73.6548	1.417	1.3912
$C_{ar.} - C_{ar.} - C_{me.}$	31.0771	47.0579	1.417	1.501
$C_{ar.} - N_{am.} - C_{al.}$	0.0000	0.0000	1.3912	0.0000
$C_{al.} - N_{am.} - C_{al.}$	0.0000	0.0000	0.0000	0.0000
$C_{ar.} - C_{al.} - C_{me.}$	0.0000	0.0000	1.5010	1.53
$H - C_{al.} - C_{me.}$	11.421	20.754	1.101	1.53
$C_{ar.} - C_{me.} - H$	26.4608	11.7717	1.501	1.1010
$H - C_{me.} - H$	18.103	18.103	1.101	1.101
$C_{al.} - C_{me.} - H$	20.754	11.421	1.53	1.101
$O_{P.} - Si_{P.} - O_{P.}$	23.438	23.438	1.6562	1.6562
$C_{al.} - Si_{P.} - O_{P.}$	6.4278	20.5669	1.9073	1.6562
$Si_{P.} - O_{P.} - Si_{P.}$	28.6686	28.6686	1.6562	1.6562
$H - C_{al.} - Si_{P.}$	14.7189	12.8694	1.101	1.9073
$C_{al.} - C_{al.} - Si_{P.}$	0.0000	0.0000	1.53	1.9073
$C_{al.} - C_{al.} - H$	20.754	11.421	1.53	1.1010
$C_{al.} - C_{al.} - O_{et.}$	2.6868	20.4033	1.53	1.42
$C_{al.} - O_{et.} - C_{al.}$	-2.8112	-2.8112	1.42	1.42
$O_{et.} - C_{al.} - C_{ep.}$	20.4033	2.6868	1.42	1.53
$H - C_{al.} - C_{ep.}$	11.421	20.754	1.101	1.53
$C_{al.} - C_{ep.} - H$	20.754	11.421	1.53	1.101
$C_{al.} - C_{ep.} - C_{ep.}$	8.016	8.016	1.53	1.53
$C_{al.} - C_{ep.} - O_{ep.}$	2.6868	20.4033	1.53	1.42
$H - C_{ep.} - C_{ep.}$	11.421	20.754	1.101	1.53
$H - C_{ep.} - O_{ep.}$	4.6189	55.327	1.101	1.42
$C_{ep.} - C_{ep.} - O_{ep.}$	2.6868	20.4033	1.53	1.42
$H - C_{ep.} - H$	18.103	18.103	1.101	1.101
$C_{ep.} - O_{ep.} - C_{ep.}$	-2.8112	-2.8112	1.42	1.42
$C_{ar.} - N_{am.} - H$	38.5704	16.5524	1.3912	1.0012
$C_{al.} - N_{am.} - H$	0.0000	0.0000	0.0000	1.0012
$H - N_{am.} - H$	17.1597	17.1597	1.0012	1.0012

*: One hydrogen is substituted with a heavy element such as a halogen or oxygen.

Table SVII Lennard-Jones potential parameters used for describing non-bond interactions. The units of ϵ_i and σ_i are kcal/mol and Å, respectively.

<i>i</i>	ϵ_i	σ_i
<i>C_{aromatic}</i>	0.064	4.01
<i>C_{alkane}</i>	0.054	4.01
<i>C_{alkane}[*]</i>	0.054	4.01
<i>C_{methyl}</i>	0.054	4.01
<i>C_{epoxide}</i>	0.054	4.01
<i>H_{C-H}</i>	0.02	2.995
<i>H_{O-H}</i>	0.013	1.098
<i>H_{N-H}</i>	0.013	1.098
<i>O_{ether}</i>	0.24	3.535
<i>O_{hydroxyl}</i>	0.24	3.535
<i>O_{epoxide}</i>	0.24	3.535
<i>O_{POSS}</i>	0.24	3.35
<i>N_{amine}</i>	0.065	4.07
<i>Si_{POSS}</i>	0.07	4.284

*: One hydrogen is substituted with a heavy element such as a halogen or oxygen.

Table SVIII Equilibrium bond length and bond dissociation energy (BDE) for the covalent bond constituting the epoxy/POSS system. The units of r_0 and BDE are Å and kcal/mol, respectively.

$i - j$	r_0	BDE	Reference
$C_{aromatic} - C_{aromatic}$	1.405	115.4	S19
$C_{aromatic} - C_{alkane}$	1.485	102.2	S20
$C_{aromatic} - H$	1.075	112.3	S20
$C_{aromatic} - O_{ether}$	1.405	101.0	S20
$C_{aromatic} - N_{amine}$	1.385	104.2	S20
$C_{aromatic} - C_{methyl}$	1.535	103.5	S20
$C_{alkane} - C_{alkane}$	1.555	87.9	S20
$C_{alkane} - H$	1.105	110.7	S20
$C_{alkane} - O_{ether}$	1.415	85.0	S20
$C_{alkane} - C_{alkane}^*$	1.505	87.9	S20
$C_{alkane} - N_{amine}$	1.355	70.75	S21
$C_{alkane} - C_{methyl}$	1.525	89.0	S20
$C_{alkane} - Si_{POSS}$	1.915	108.0	S22
$C_{alkane} - C_{epoxide}$	1.515	87.9	S23

$C_{alkane}^* - H$	1.085	97.1	S20
$C_{alkane}^* - O_{hydroxyl}$	1.435	94.0	S20
$C_{methyl} - H$	1.095	104.9	S20
$C_{epoxide} - C_{epoxide}$	1.485	88.5	S23
$C_{epoxide} - O_{epoxide}$	1.465	54.0	S23
$C_{epoxide} - H$	1.085	104.9	S20
$O_{hydroxyl} - H_{hydroxyl}$	0.965	101.1	S20
$N_{amine} - H$	1.005	89.1	S24
$Si_{POSS} - O_{POSS}$	1.715	191.2	S22

*: One hydrogen is substituted with a heavy element such as a halogen or oxygen.

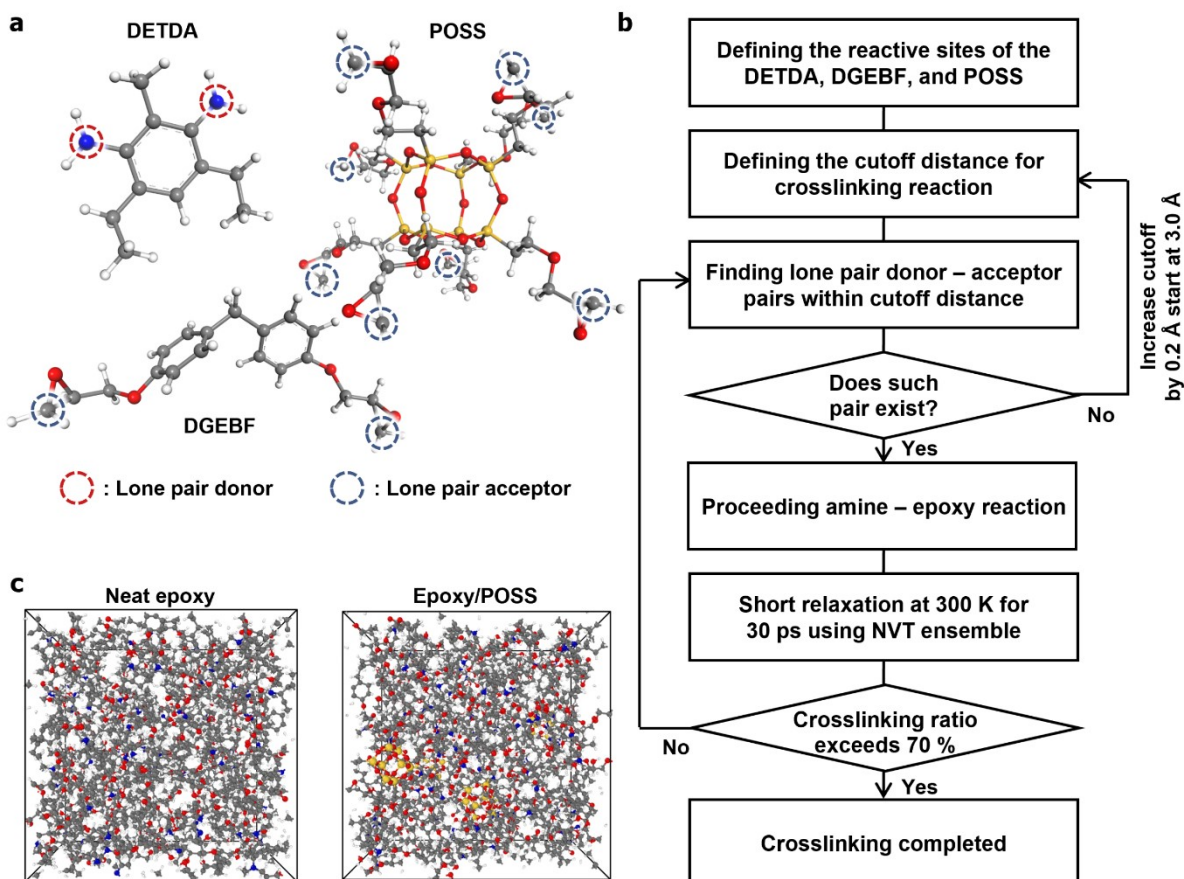


Figure S1 All-atom modeling process of crosslinked neat epoxy and epoxy/POSS nanocomposites. **a.** Molecular structure of DETDA, DGEBF, and octa(3-Glycidyl)propoxy POSS. The lone pair donors and acceptors (i.e., the reactive sites) are highlighted in the red and blue circles, respectively. **b.** The workflow of the formation of crosslinks between molecules constituting the microstructure. The initial cutoff distance was set at 3.0 Å and the value was gradually increased in steps of 0.2 Å until the crosslinking ratio of the entire epoxy system reached 70%. By changing the cutoff value in such a small and delicate manner, the covalent bonds of the C–N pairs newly formed by the cross-linking were prevented from drastically changing the potential energy of the entire system and the shape of the network. **c.** Configurations of crosslinked neat epoxy and epoxy/POSS nanocomposites unit cells after the MD equilibration.

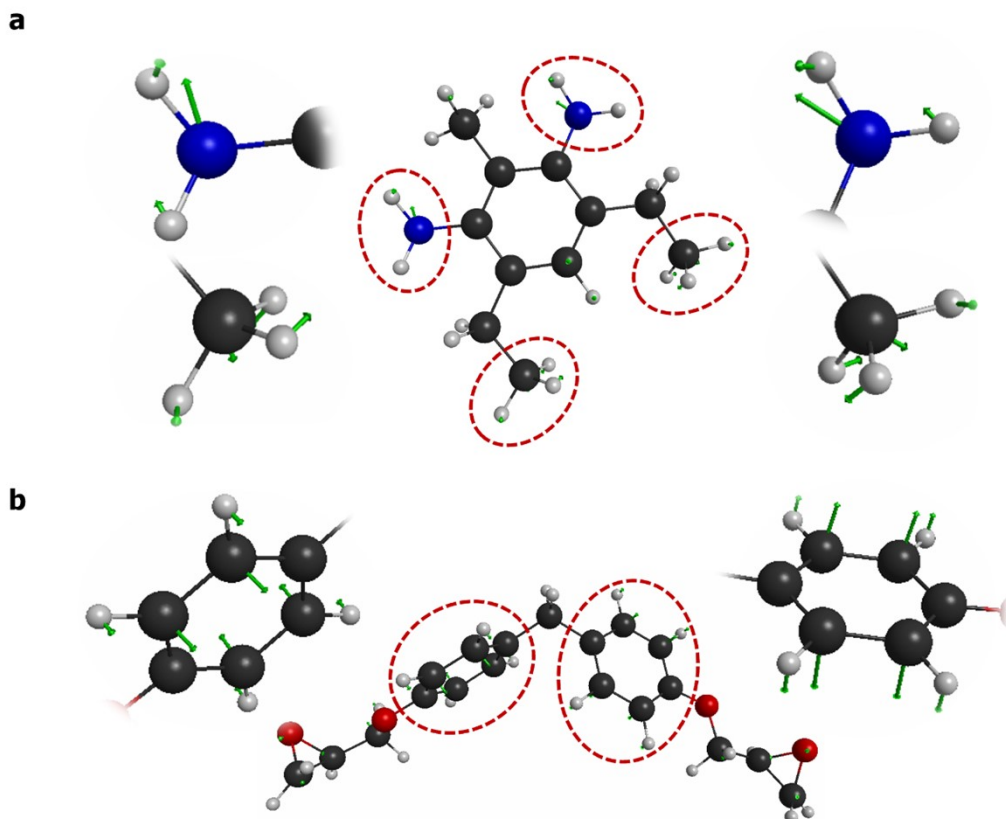


Figure S2 Activated normal modes under deep-UV. **a.** ν_{13}^1 state of DETDA. **b.** ν_1^1 state of DGEBF.

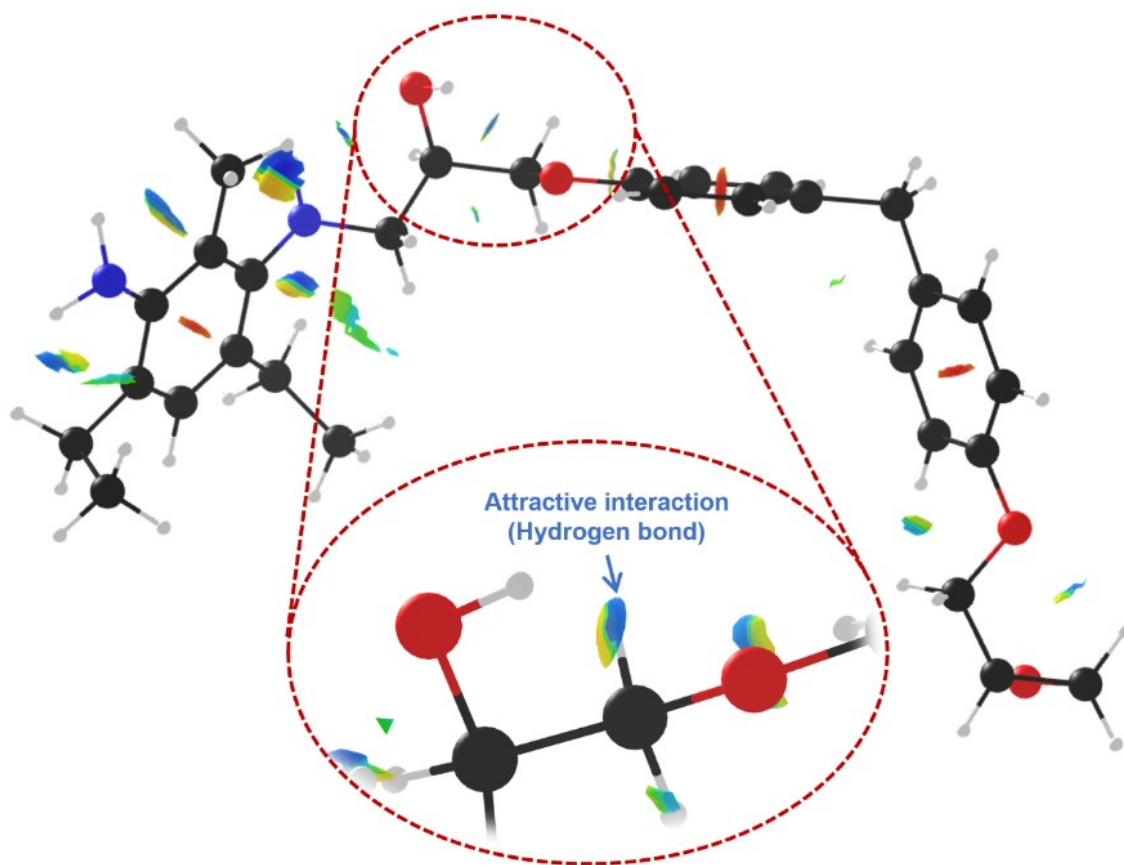


Figure S3 Distribution of non-covalent interaction energy of the crosslinked epoxy. Colored surfaces in the voids between atoms exhibit attractive (blue) and repulsive (red) interaction potentials.^{S25, S26} The molecular structure of the crosslinked epoxy is optimized at B3LYP/6-31G(d)+ level.^{S16, S17}

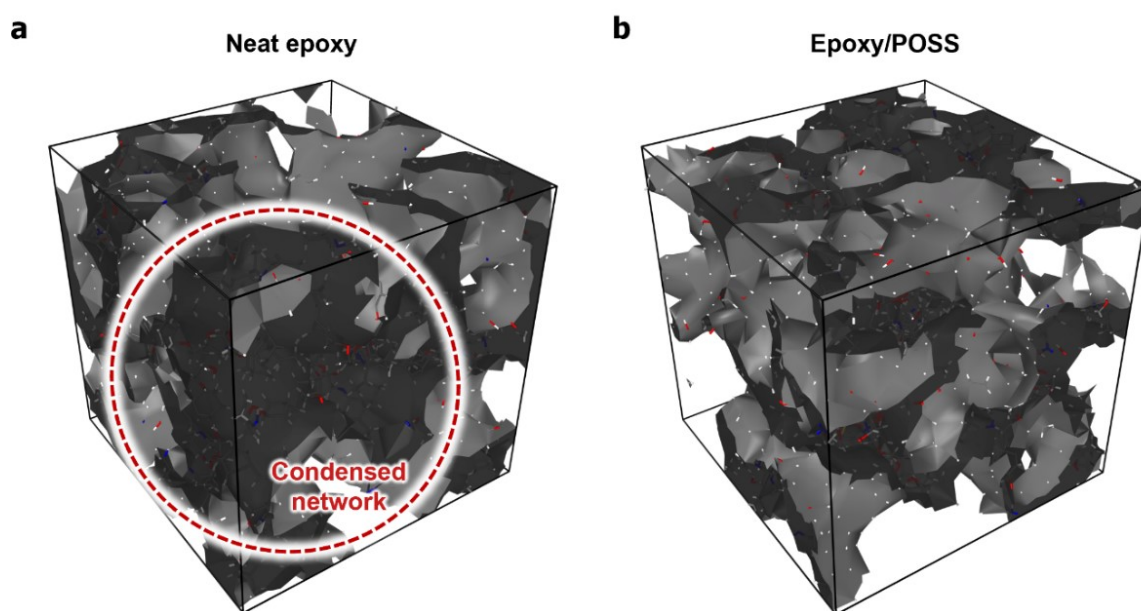


Figure S4 Deteriorated network structure of **a.** the neat epoxy and **b.** the epoxy/POSS nanocomposites after UV irradiation. Morphology of the network structures is visualized by the Connolly surface analysis using a probe sphere radius of 3 Å. Only the atoms constituting the network are shown for visibility.

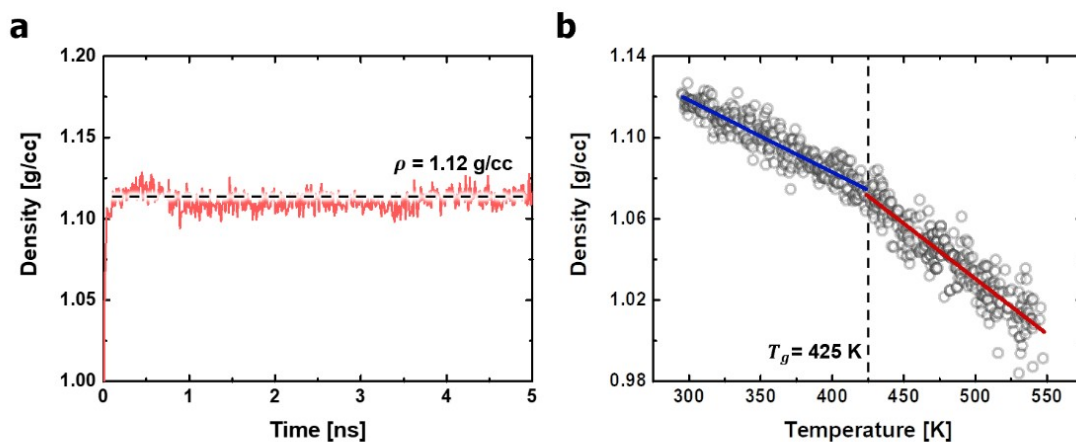


Figure S5 Physical properties of neat epoxy predicted by classical MD simulations used in this study: **a.** density (ρ), and **b.** glass transition temperature (T_g).

References

- [S1] S. Plimpton, Fast parallel algorithms for short-range molecular dynamics. *J. Comp. Phys.* **117** (1995) 1–19.
- [S2] H. Sun, Force field for computation of conformational energies, structures, and vibrational frequencies of aromatic polyesters. *J. Comput. Chem.* **15** (1994) 752-768.
- [S3] A. Vashisth, C. Ashraf, W. Zhang, C. E. Bakis, A. C. T. van Duin, Accelerated ReaxFF Simulations for Describing the Reactive CrossLinking of Polymers. *J. Phys. Chem. A* **122** (2018) 6633-6642.
- [S4] G. M. Odegard, S. U. Patil, P. P. Deshpande, K. Kanhaiya, J. J. Winetrou, H. Heinz, S. P. Shah, M. Maiaru, Molecular Dynamics Modeling of Epoxy Resins Using the Reactive Interface Force Field. *Macromolecules* **54** (2021) 9815-9824.
- [S5] S. Wang, Z. Liang, P. Gonnet, Y.-H. Liao, B. Wang, C. Zhang, Effect of Nanotube Functionalization on the Coefficient of Thermal Expansion of Nanocomposites. *Adv.*

Funct. Mater. **17** (2007) 87-92.

- [S6] J. Choi, H. Shin, S. Yang, M. Cho, The influence of nanoparticle size on the mechanical properties of polymer nanocomposites and the associated interphase region: A multiscale approach. *Compos. Struct.* **119** (2015) 365-376.
- [S7] C. Li, A. Strachan, Molecular dynamics predictions of thermal and mechanical properties of thermoset polymer EPON862/DETDA. *Polymer* **52** (2011) 2920-2928.
- [S8] J. Cho, C. T. Sun, A molecular dynamics simulation study of inclusion size effect on polymeric nanocomposites. *Comput. Mater. Sci.* **41** (2007) 54-62.
- [S9] H. Dammak, Y. Chalopin, M. Laroche, M. Hayoun, J.-J. Greffet, Quantum Thermal Bath for Molecular Dynamics Simulation. *Phys. Rev. Lett.* **103** (2009) 190601.
- [S10] H. B. Callen, T. A. Welton, Irreversibility and Generalized Noise. *Phys. Rev.* **83** (1951) 34-40.
- [S11] F. Calvo, C. Falvo, P. Parneix, Atomistic Modeling of Vibrational Action Spectra in Polyatomic Molecules: Nuclear Quantum Effects. *J. Phys. Chem. A* **118** (2014) 5427-5436.
- [S12] F. Briec, Y. Bronstein, H. Dammak, P. Depondt, F. Finocchi, M. Hayoun, Zero-Point Energy Leakage in Quantum Thermal Bath Molecular Dynamics Simulations. *J. Chem. Theory Comput.* **12** (2016) 5688-5697.
- [S13] T. Qi, E. J. Reed, Simulations of Shocked Methane Including Self-Consistent Semiclassical Quantum Nuclear Effects. *J. Phys. Chem. A* **116** (2012) 10451-10459.
- [S14] G. Li, P. Hu, W. Luo, J. Zhang, H. Yu, F. Chen, F. Zhang, Simulation of pyrolysis of crosslinked epoxy resin using ReaxFF molecular dynamics. *Comput. Theor. Chem.* **1200** (2021) 113240.
- [S15] M. W. Schmidt, K. K. Baldridge, J. A. Boatz, S. T. Elbert, M. S. Gordon, J. H. Jensen,

- S. Koseki, N. Matsunaga, K. A. Nguyen, S. J. Su, T. L. Windus, M. Dupuis, J. A. Montgomery Jr., General atomic and molecular electronic structure system. *J. Comput. Chem.* **14** (1993) 1347–1363.
- [S16] A. D. Becke, Density-functional thermochemistry. III. The role of exact exchange. *J. Chem. Phys.* **98** (1993) 5648.
- [S17] C. Lee, W. Yang, R. G. Parr, Development of the Colle-Salvetti correlation-energy formula into a functional of the electron density. *Phys. Rev. B* **37** (1988) 785–789.
- [S18] Y. Kim, J. Choi, Theoretical Study on the Pyrolysis Process of POSS Nanocomposites Based on the Molecular Vibration Frequency. *Under review*.
- [S19] S. Fitzsár, Atoms, Chemical Bonds and Bond Dissociation Energies. Springer-Verlag, (1994).
- [S20] S. J. Blanksby, G. B. Ellison, Bond Dissociation Energies of Organic Molecules. *Acc. Chem. Res.* **36** (2003) 255-263.
- [S21] Y.-R. Luo, Comprehensive Handbook of Chemical Bond Energies. CRC Press, (2007).
- [S22] B. H. Augustine, Wm. C. Hughes, K. J. Zimmermann, A. J. Figueiredo, X. Guo, C. C. Chusuei, J. S. Maidment, Plasma Surface Modification and Characterization of POSS-Based Nanocomposite Polymeric Thin Films. *Langmuir* **23** (2007) 4346-4350.
- [S23] A. Manakhov, Š. Fuková, D. Nečas, M. Michlíček, S. Ershov, M. Eliaš, M. Visotin, Z. Popov, L. Zajíčková^{abc}, Analysis of epoxy functionalized layers synthesized by plasma polymerization of allyl glycidyl ether. *Phys. Chem. Chem. Phys.* **20** (2018) 20070-20077.
- [S24] L. Ji, G. Schüürmann, Model and Mechanism: N-Hydroxylation of Primary Aromatic Amines by Cytochrome P450. *Angew. Chem.-Int. Edit.* **52** (2013) 744-748.
- [S25] E. R. Johnson, S. Keinan, P. Mori-Sánchez, J. Contreras-García, A. J. Cohen, W. Yang,

Revealing noncovalent interactions. *J. Am. Chem. Soc.* **132** (2010) 6498-6506.

- [S26] Y. Kim, J. Choi, Chemo-mechano-structural interplay in fully hydrated ion clusters on hexagonal boron nitride nanosheet surfaces. *Mater. Today Chem.* **26** (2022) 101161.